Fast Fluoride Ion Conduction in Molecular Cation-Containing Compounds, $NH_4(Mg_{1-x}Li_x)F_{3-x}$ and $(NH_4)_2(Mg_{1-x}Lix)F_{4-x}$

Kota Motohashi (kota.motohashi@chem.osakafu-u.ac.jp)
Tohoku University
Yosuke Matsukawa
Tohoku University
Takashi Nakamura
Tohoku University
Yuta Kimura
Tohoku University
Yoshiharu Uchimoto
Kyoto University
Koji Amezawa
Tohoku University

Research Article

Keywords: conductors, fluoride, flexible, molecular

Posted Date: October 28th, 2021

DOI: https://doi.org/10.21203/rs.3.rs-1003032/v1

Abstract

Aiming development of the fast anion conductors, we proposed a new material design using flexible molecular cation as a host cation, and demonstrated it with fluoride ion conduction in $NH_4(Mg_{1-x}Li_x)F_{3-x}$ and $(NH_4)_2(Mg_{1-x}Li_x)F_{4-x}$. Relatively high fluoride ion conductivities of 4.8×10^{-5} S cm^{-1} and 8.4×10^{-6} S cm^{-1} were achieved at 323 K in $(NH_4)_2(Mg_{0.85}Li_{0.15})F_{3.85}$ and $NH_4(Mg_{0.9}Li_{0.1})F_{2.9}$, respectively. Our findings suggest molecular cation-containing compounds can be attractive material groups for fast anion conductors.

Introduction

Developing high energy density batteries are an urgent issue for establishing environmentally-friendly and sustainable society. All-solid-state fluoride ion batteries (ASSFIBs) are one of promising batteries because of their potential of high energy density.[1–4] The energy density of ASSFIBs is theoretically expected to reach 5000 Wh L^{-1}. However, state-of-the-art ASSFIBs still have many problems, for instance, the gap between theoretical and practical discharge/charge capacities, the poor cycling performance, the high operating temperature, the insufficient operating voltage, and so on.[5,6] One major reason for such poor performances of the present ASSFIBs is the lack of suitable solid electrolytes having high ionic conductivity and thermochemical stability. $PbSnF_4$ shows the highest ionic conductivity, 1.6×10^{-3} S cm^{-1} at room temperature, among already-known solid-state fluoride ion conductors. However, this material is unstable under the high operating voltage due to the narrow potential window.

There are several strategies for development of solid electrolytes. One is the use of highly disordered structure advantageous for high ionic conduction. Another is the introduction of the mobile ionic defects (such as vacancies or interstitial ions) by doping aliovalent ions. Among fluoride ion conductors, $PbSnF_4$, $RbSnF_3$, and b-PbF_2 are the materials developed based on the former strategy.[7–10] On the other hand, the tysonite-type $La_{1-x}Ba_xF_{3-x}$ and $Sm_{1-x}Ca_xF_{3-x}$ and the fluorite-type $Sn_{1-x}K_xF_{2-x}$ and $Ba_{1-x}La_xF_{2+x}$ are the materials based on the latter one.[11–14] Although various fluoride ion conductors are previously reported,[15,16] further material explorations for sufficiently high fluoride ion conductivity are required to realize ASSFIBs.

Excellent cation conduction has been reported in some materials containing molecular anions such as PO_4^{3-}, SiO_4^{4-}, PS_4^{3-}, and *etc.*. proton conductors like CsH_2PO_4 and lithium ion conductors like Li_3PO_4-Li_4SiO_4 and Li_3PS_4 are the typical examples.[17–20] High cation conductivity in these materials is considered to be caused by unique size, structure, and dynamics of molecular ions, resulting in extension of the bottleneck for ion conduction, reduction of the interaction between the host and carrier ions, and assistance of the ion conduction by the rotation of the molecular ions[21], and so on. Considering these, a similar strategy can be applied to develop novel anion conductors. There had been some attempts to develop new fluoride ion conductors containing molecular ions such as NH_4^+ in NH_4SnF_3.[22] However, the

role of molecular cations for anion conduction has not been well examined. It is therefore interesting to systematically investigate the potential of materials containing molecular cations as fast anion conductors.

In this study, perovskite and layered perovskite fluorides containing NH_4^+ as a molecular cation, NH_4MgF_3 and $(NH_4)_2MgF_4$, are selected as targets of materials.[23] $NH_4(Mg_{1-x}Li_x)F_{3-x}$ and $(NH_4)_2(Mg_{1-x}Li_x)F_{4-x}$ were prepared with the intention of introducing fluoride ion vacancies by the substitution of Li^+ for Mg^{2+}, and their electrical conduction properties were studied. In comparison, the conductivities of perovskite and layered perovskite containing K^+ as the A-site cation, $K(Mg_{0.9}Li_{0.1})F_{2.9}$ and $K_2(Mg_{0.9}Li_{0.1})F_{3.9}$, were examined. Since the ionic radius of K^+ (1.64 Å) is similar to the effective radius of NH_4^+ (1.46 Å),[24] the influence of the molecular ions on the ionic conductivity can be discussed.

$NH_4(Mg_{1-x}Li_x)F_{3-x}$ and $(NH_4)_2(Mg_{1-x}Li_x)F_{4-x}$ were synthesized by solid state reaction methods. The obtained powders and pressed compacts were characterized by X-ray diffraction (XRD), scanning electron microscopy (SEM) observation, and electron probe micro analyzer (EPMA). The thermal stabilities of NH_4MgF_3 and $(NH_4)_2MgF_4$ were examined by thermogravimetry (TG). The electrical conductivities of the compacts were measured by AC electrochemical impedance spectroscopy (EIS). To confirm the dominant fluoride ion conduction, AC EIS and DC polarization measurements were performed with the fluoride ion conducting cell. In order to cross-check the dominant fluoride ion conduction, electromotive force (*emf*) measurements of the fluorine concentration cell, M_1F_x-M_1/sample/M_2F_x-M_2 ($M_{1,2}$: metal, $M_{1,2}F_{x,x}$: metal fluoride), were performed.

Results

Figures 1 (a) and (b) show the XRD patterns of (a) $NH_4(Mg_{1-x}Li_x)F_{3-x}$ and (b) $(NH_4)_2(Mg_{1-x}Li_x)F_{4-x}$. The most of XRD peaks could be indexed with the cubic ($Pm\bar{3}m$) symmetry for $NH_4(Mg_{1-x}Li_x)F_{3-x}$ and the tetragonal symmetry ($I4/mmm$) for $(NH_4)_2(Mg_{1-x}Li_x)F_{4-x}$. In $NH_4(Mg_{1-x}Li_x)F_{3-x}$, the diffraction peaks of the cubic phase gradually shifted to lower angle with increasing the Li content. This indicated that larger Li^+ (0.76 Å) was substituted into the smaller Mg^{2+} (0.72 Å) sites. The lattice parameters of $NH_4(Mg_{1-x}Li_x)F_{3-x}$ and $(NH_4)_2(Mg_{1-x}Li_x)F_{4-x}$ were calculated from the diffraction angles and were plotted in Figs. 1 (c) and (d) as a function of the Li content. Except for the *c*-axis of $(NH_4)_2(Mg_{1-x}Li_x)F_{4-x}$, the lattice parameters changed monotonically with the Li content in $NH_4(Mg_{1-x}Li_x)F_{3-x}$ and $(NH_4)_2(Mg_{1-x}Li_x)F_{4-x}$ phases, suggesting that solid solution is formed at least within the compositional range of $0 < x < 0.3$ in $NH_4(Mg_{1-x}Li_x)F_{3-x}$ and $0 < x < 0.2$ in $(NH_4)_2(Mg_{1-x}Li_x)F_{4-x}$ and the solubility limit of Li is higher than 30 mol% in $NH_4(Mg_{1-x}Li_x)F_{3-x}$ and 20 mol% in $(NH_4)_2(Mg_{1-x}Li_x)F_{4-x}$. Small diffraction peaks of NH_4NO_3 could be found in some compositions, especially in $NH_4(Mg_{0.8}Li_{0.2})F_{2.8}$. In order to investigate the state and location of the impurity, the SEM observation and EPMA analysis were carried out. The results for $NH_4(Mg_{0.8}Li_{0.2})F_{2.8}$ were presented in Figs. S1. The impurity, possibly NH_4NO_3, was observed as indicated

by the yellow circles in Fig. S1. However, since the impurity particles seemed to exist sparsely from the main compound and their amount was not significant, the influences of the impurity on the observed ionic conductivities were supposed as negligibly small.

The SEM images of the cross sections of the pressed compacts of $NH_4(Mg_{0.8}Li_{0.2})F_{2.8}$ and $(NH_4)_2(Mg_{0.85}Li_{0.15})F_{3.85}$ were shown in Fig. S2. The compacts seemed dense as just pressed compact, and the relative densities of all the compacts were approximately 75 %.

Figure S3 (a) and (b) show the results of TG measurement. NH_4MgF_3 and $(NH_4)_2(Mg_{0.8}Li_{0.2})F_{3.8}$ were stable below approximately 443 and 413 K, respectively. As shown in Figs. S3 (c) amd (d), XRD analysis indicated that NH_4MgF_3 was decomposed to MgF_2 at around 443 K and $(NH_4)_2MgF_4$ was decomposed into NH_4MgF_3 and MgF_2 near 413 K forming NH_4F gas.

Figures 2 show Nyquist plots observed with (a) $NH_4(Mg_{1-x}Li_x)F_{3-x}$ and (b) $(NH_4)_2(Mg_{1-x}Li_x)F_{4-x}$ at 323 K. Although the results are not given in Figs. 2, only scattered signals were observed in EIS measurements with non-doped NH_4MgF_3, indicating its extremely low electrical conductivity. On the other hand, the Li-doped samples showed typical impedance responses of an ionic conductor with blocking electrodes, *e.g.* a semicircle in the high frequency region and a sharp spike in the low frequency region. These impedance behaviours suggested ionic conductivity in these samples. The resistance of the sample was determined from the semicircle in high frequency region. Figure 3 shows temperature dependences of the electrical conductivities of $NH_4(Mg_{1-x}Li_x)F_{3-x}$ and $(NH_4)_2(Mg_{1-x}Li_x)F_{4-x}$. The conductivities were enhanced by Li-doping, but they showed the maximum and decreased with further increasing the Li content. At 323 K, the maximum conductivity was observed at $x = 0.1$ for $NH_4(Mg_{1-x}Li_x)F_{3-x}$ (8.4×10^{-6} S cm^{-1}) and at $x = 0.15$ for $(NH_4)_2(Mg_{1-x}Li_x)F_{4-x}$ (4.8×10^{-5} S cm^{-1}). The decrease in electrical conductivity in highly doped samples is considered to be caused by cluster formation or ordering of fluoride ions and vacancies, and *etc.*.[25,26]

In order to confirm dominant fluoride ion conduction in the investigated materials, we prepared a blocking cell consisting of Pb/$PbSnF_4$/sample/$PbSnF_4$/Pb. Since $PbSnF_4$ is an almost pure fluoride ion conductor, this cell conducts only fluoride ion under steady-state DC bias, while the AC conductivity of the cell includes the contribution of all mobile carriers in the sample. Thus, if the conductivities measured by AC EIS and DC polarization methods are comparable, it can be concluded the dominant carrier is fluoride ion. The voltage transient curves observed in DC polarization measurements with a Pb/$PbSnF_4$/samples/$PbSnF_4$/Pb at various temperatures are shown in Figs. S4 (b)-(e) and S5 (b)-(h). The measured voltages were considerably increased immediately after the DC polarization and then gradually increased with time. From the impedance spectra shown in Figs. S4(a) and S5(a), the relaxation times for electrical conduction in $NH_4(Mg_{0.9}Li_{0.1})F_{2.9}$ and $(NH_4)_2(Mg_{0.95}Li_{0.05})F_{3.95}$ were faster than 10^{-1} s. Thus, the gradual increase of the voltage might be mainly caused by the formation of resistive interphases by the decomposition of $PbSnF_4$ at the $PbSnF_4$/current-corrector interface. Therefore, the DC conductivity of the blocking cell was evaluated from the current and the voltage drop observed at 1 second after applying DC current. Figure 4 shows temperature dependence of conductivities of

$NH_4(Mg_{0.9}Li_{0.1})F_{2.9}$ and $(NH_4)_2(Mg_{0.95}Li_{0.05})F_{3.95}$ measured by AC EIS and DC polarization methods with a Pb/$PbSnF_4$/sample/$PbSnF_4$/Pb cell. The conductivities by AC EIS and DC polarization methods were comparable both $NH_4(Mg_{0.9}Li_{0.1})F_{2.9}$ and $(NH_4)_2(Mg_{0.95}Li_{0.05})F_{3.95}$. Thus, it can be concluded that the dominant carrier was fluoride ion both in $NH_4(Mg_{1-x}Li_x)F_{3-x}$ and $(NH_4)_2(Mg_{1-x}Li_x)F_{4-x}$.

In Fig. 3, the conductivities of conventional fluoride ion conductors are shown by dash-dotted lines[3, 27–29]. The fluorides investigated in this work exhibited relatively high ionic conductivity, although not as high as that of the best fluoride ion conductor, $PbSnF_4$. It is also noteworthy that pressed compacts of $NH_4(Mg_{1-x}Li_x)F_{3-x}$ and $(NH_4)_2(Mg_{1-x}Li_x)F_{4-x}$ showed relatively high conductivities without sintering. This can be a great advantage for the fabrication of all-solid-state batteries. The activation energies of $NH_4(Mg_{1-x}Li_x)F_{3-x}$ and $(NH_4)_2(Mg_{1-x}Li_x)F_{4-x}$ were approximately 1.0 eV, as summarized in Table S1. The activation energies of $NH_4(Mg_{1-x}Li_x)F_{3-x}$ and $(NH_4)_2(Mg_{1-x}Li_x)F_{4-x}$ were slightly higher than those of the reported typical fluoride ion conductors.

In the case of the layered perovskite structure, interstitial anions sometimes can be mobile, as interstitial oxygens in Ln_2NiO_{4+d} (Ln = rare earth).[30] Based on this idea, the introduction of interstitial fluoride ions was tried for the layered perovskite $(NH_4)_2MgF_4$ by partially substituting trivalent cation Sc^{3+} for Mg^{2+}. However, as shown in Fig. S6, this trial was not effective for improving the ionic conductivity of $(NH_4)_2MgF_4$.

In order to demonstrate the influence of the molecular cations on the anionic conductivity, $K(Mg_{0.9}Li_{0.1})F_{2.9}$ having the same crystal structures was prepared. The lattice constant of $K(Mg_{0.9}Li_{0.1})F_{2.9}$ was 3.989 Å which was comparable with $NH_4(Mg_{0.9}Li_{0.1})F_{2.9}$, 4.072 Å. The electrical conductivities of $K(Mg_{0.9}Li_{0.1})F_{2.9}$ and $K_2(Mg_{0.9}Li_{0.1})F_{3.9}$ were considerably low, 5.2×10^{-6} S cm^{-1} at 789 K and 7.3×10^{-5} S cm^{-1} at 717 K, respectively (Fig. S7). Although the reason for the conductivity enhancement by the substitution of K^+ for NH^{4+} is not clear at this moment, extension of the bottleneck for ion conduction, reduction of the interaction between the host and carrier ions, or assistance of the ion conduction by the rotation of the molecular ions might occur, as in fact cation conductors containing molecular anions. In this work, we succeeded to achieve relatively high fluoride ion conductivity in compounds containing molecular cations, $NH_4(Mg_{1-x}Li_x)F_{3-x}$ and $(NH_4)_2(Mg_{1-x}Li_x)F_{4-x}$, by introducing fluoride ion vacancies. The findings of this works suggested that compounds containing molecular cations can be new host materials for fast anion conductors.

Conclusion

$NH_4(Mg_{1-x}Li_x)F_{3-x}$ and $(NH_4)_2(Mg_{1-x}Li_x)F_{4-x}$ were found to exhibit relatively high fluoride ion conductivities of 8.4×10^{-6} (x = 0.1) and 4.8×10^{-5} (x = 0.15) S cm^{-1} at 323 K, respectively. The major conduction carrier was identified as fluoride ion. This work demonstrated that compounds containing molecular cations, like

hybrid organic-inorganic perovskites, can be a promising material group for noble anion-conducting materials.

Methods

Synthesis and characterization

$NH_4(Mg_{1-x}Li_x)F_{3-x}$ and $(NH_4)_2(Mg_{1-x}Li_x)F_{4-x}$ were synthesized from $3MgCO_3{\bullet}3H_2O$ (99.9 %, Kojundo Chemical Laboratory Co., LTD., Japan), NH_4F (97.0+ %, Wako Pure Chemical Industries, Ltd., Japan) and $LiNO_3$ (99.9 %, Wako Pure Chemical Industries, Ltd., Japan) by a solid state reaction. For the synthesis of the compounds, excess amount of NH_4F was required to compensate the evaporation of NH_4F during the calcination. Figure S8 shows the products obtained with different molar ratios of NH_4MgF_3. When the mixing ratio was 1:7, the single phase of the perovskite NH_4MgF_3 was obtained, while impurities including MgF_2 were observed with the mixing ratios below 1 : 6, suggesting the lack of NH_4^+. Considering these results, raw material powders were mixed with a molar ratio of Mg : Li : F = (1-x) : x : 7. The mixture was calcined at 453 K for $NH_4(Mg_{1-x}Li_x)F_{3-x}$ and 433 K for $(NH_4)_2(Mg_{1-x}Li_x)F_{4-x}$ for 2 - 8 hours under Ar gas flow. In order to remove remaining NH_4F, the mixtures were additionally calcined at 433 K for $NH_4(Mg_{1-x}Li_x)F_{3-x}$ and 413 K for $(NH_4)_2(Mg_{1-x}Li_x)F_{4-x}$ for 1 - 5 hours.

$K(Mg_{0.9}Li_{0.1})F_{2.9}$ $K_2(Mg_{0.9}Li_{0.1})F_{3.9}$ were synthesized from KF (99 %, Wako Pure Chemical Industries, Ltd., Japan), MgF_2 (99.9 % up, Kojundo Chemical Laboratory Co., LTD., Japan), and LiF (99.98 %, Sigma-Aldrich Japan, Japan) by solid state reaction. Powders of reagents were mixed in a stoichiometric ratio, and milled in Ar atmosphere by a planetary ball milling (P-6, Fritsch Japan Co., Ltd., Japan) at 600 rpm for 12 h. The mixtures were sintered at 923 K for $K(Mg_{0.9}Li_{0.1})F_{2.9}$ and 873 K for $K_2(Mg_{0.9}Li_{0.1})F_{3.9}$ for 10 h in Ar atmosphere.

The obtained samples were characterized by X-ray diffraction (XRD, D2 phaser, Bruker AXS, Germany), scanning electron microscopy observation (SEM, JSM-7800F, JEOL, Japan), and electron probe micro analyzer (EPMA, JXA-8530F, JEOL, Japan). The thermal stability of the obtained samples was evaluated by thermogravimetry (TG, Cahn D200, Thermo Fisher Scientific K. K., Japan).

Electrical conductivity measurements

The obtained $NH_4(Mg_{1-x}Li_x)F_{3-x}$ and $(NH_4)_2(Mg_{1-x}Li_x)F_{4-x}$ powders were pelletized at 200 MPa by a cold isostatic pressing method. Au thin film electrodes were sputtered on the both sides of the dense pellets. Electrical conductivities were evaluated from AC electrochemical impedance spectroscopy (EIS) at 303 - 343 K in N_2 gas with 30 - 50 mV of amplitude with frequency of $4.0{\times}10^7$ to 1 Hz by using the impedance analyzer (Alpha-A, Novocontrol Technologies GmbH & Co. KG, Germany).

The powders of $K(Mg_{0.9}Li_{0.1})F_{2.9}$ and $K_2(Mg_{0.9}Li_{0.1})F_{3.9}$ were pelletized at 200 MPa by a uniaxial pressure, and sintered at 1073 or 873 K for 10 hours. Electrical conductivities of $K(Mg_{0.9}Li_{0.1})F_{2.9}$ and

$K_2(Mg_{0.9}Li_{0.1})F_{3.9}$ were evaluated from AC EIS at room temperature - 788 K in Ar atmosphere by using a potentiostat (VersaSTAT, Princeton Applied Research, USA).

To confirm the dominant fluoride ion conduction, DC polarization measurements were performed by using the blocking cell consisting of $Pb/PbSnF_4/sample/PbSnF_4/Pb$ at room temperature - 423 K under vacuum. Schematic illustration of the blocking cell was given in Fig. S9. The current for DC polarization measurements was 10 or 20 mA.

Declarations

[Acknowledgements]

This work was partly supported by JST-Mirai Program JPMJMI18E2 and Grant-in-Aid for JSPS Fellow Grant number 20J12230, Japan.

[Author contributions]

K.M. contributed the following: funding acquisition, investigation, data curation, and writing original draft. Y. M. performed the experiments. T. N., and Y. K. discussed the results and wrote - review and editing manuscript. Y. U. prepared the measurement environment. K.A. contributed the following: conceptualization, funding acquisition, resources, and writing – review and editing. The ideas and experiments were conceived, planned, and analyzed by all co-authors under the supervision of K. A. All the authors have given approval to the final version of the manuscript.

[Additional information]

Supplementary information accompanies this paper at ~~~~~~~.

Competing financial interests: The authors declare no competing financial interests.

References

1. Reddy, M. A., & Fichtner, M., Batteries based on fluoride shuttle. J. Mater. Chem. 21,17059–17062, *DOI*: https://doi.org/10.1039/C1JM13535J *(*2011*).*
2. Gschwind, F., *et al*., Fluoride ion batteries: Theoretical performance, safety, toxicity, and a combinatorial screening of new electrodes. J. Fluor. Chem. 182,76–90, *DOI*: https://doi.org/10.1016/j.jfluchem.2015.12.002 *(*2016*).*
3. Rongeat, C., Reddy, M. A., Witter, R., & Fichtner, M., Nanostructured Fluorite-Type Fluorides As Electrolytes for Fluoride Ion Batteries. J. Phys. Chem. C. 117,4943–4950, *DOI*: https://doi.org/10.1021/jp3117825 *(*2013*).*
4. Zhang, D., *et al*., Understanding the reaction mechanism and performance of 3d transition metal cathodes for all-solid-state fluoride ion batteries. J. Mater. Chem. A. 9,406–412, *DOI*:

https://doi.org/10.1039/D0TA08824B (2021).

5. Mohanmmad, I., Witter, R., Fichtner, M., & Reddy, M. A., Room-Temperature, Rechargeable Solid-State Fluoride-Ion Batteries. ACS Appl. Energy Mater. 1,4766–4775, *DOI*: https://doi.org/10.1021/acsaem.8b00864 (2018).
6. Bhatia, H., *et al.*, Conductivity Optimization of Tysonite-type La1-xBaxF3-x Solid Electrolytes for Advanced Fluoride Ion Battery. ACS Appl. Mater. Interfaces. 9,23707–23715, *DOI*: https://doi.org/10.1021/acsami.7b04936 (2017).
7. Hull, S., Superionics: crystal structures and conduction processes. Rep. Prog. Phys. 67,1233, *DOI*: https://doi.org/10.1088/0034-4885/67/7/R05 (2004).
8. Yamane, Y., Yamada, K., & Inoue, K., Mechanochemical synthesis and order-disorder phase transition in fluoride ion conductor RbPbF3. Solid State Ionics. 179,605–610, *DOI*: https://doi.org/10.1016/j.ssi.2008.04.022 (2008).
9. Réau, J., *et al.*, Etude des proprietes structurales et electrioues d'un nouveau conducteur anionique: PbSnF4. Mater. Res. Bull. 13,877–882, *DOI*: https://doi.org/10.1016/0025-5408(78)90097-1 (1978).
10. Murakami, M., *et al.*, High Anionic Conductive Form of PbxSn2-xF4. Chem. Mater. 31,7704–7710, *DOI*: https://doi.org/10.1021/acs.chemmater.9b02623 (2019).
11. Rongeat, C., Reddy, M. A., *Witter*, & *R.*, Fichtner., Solid Electrolytes for Fluoride Ion Batteries: Ionic Conductivity in Polycrystalline Tysonite-Type Fluorides. ACS Appl. Mater. Interfaces. 6,2103–2110, *DOI*: https://doi.org/10.1021/am4052188 (2014).
12. Dieudonné, B., *et al.*, Exploring the Sm1-xCaxF3-x Tysonite Solid Solution as a Solid-State Electrolyte: Relationships between Structural Features and F- Ionic Conductivity. J. Phys. Chem. C. 119,25170–25179, *DOI*: https://doi.org/10.1021/acs.jpcc.5b05016 (2015).
13. Patro, L. N., Hariharan, K., Ionic transport studies in Sn(1-x)KxF(2-x) type solid electrolytes. Mater. Res. Bull.47,2492–2497, *DOI*: https://doi.org/10.1016/j.materresbull.2012.05.006 (2012).
14. Düvel, A., Bednarcik, J., Šepelák, V., & Heitjans, P., Mechanosynthesis of the Fast Fluoride Ion Conductor Ba1-xLaxF2+x: From the Fluorite to the Tysonite Structure. J. Phys. Chem. C. 118,7117–7129, *DOI*: https://doi.org/10.1021/jp410018t (2014).
15. Motohashi, K., Nakamura, T., Kimura, Y., Uchimoto, Y., & Amezawa, K., Influence of microstructures on conductivity in Tysonite-type fluoride ion conductors. Solid State Ionics.338,113–120, *DOI*: https://doi.org/10.1016/j.ssi.2019.05.023 (2019).
16. Patro, L. N., Hariharan, K., Fast fluoride ion conducting materials in solid state ionics: An overview. Solid State Ionics. 239,41–49, *DOI*: https://doi.org/10.1016/j.ssi.2013.03.009 (2013).
17. Baranov, A. I., Khiznichenko, V. P., Sandler, V. A., & Shuvalov, L. A., Frequency dielectric dispersion in the ferroelectric and superionic phases of CsH2PO4.Ferroelectrics.81,183–186, *DOI*: https://doi.org/10.1080/00150198808008840 (1988).
18. Hu, Y. W., Raistrick, I. D., & Huggins, R. A., Ionic Conductivity of Lithium Orthosilicate-Lithium Phosphate Solid Solutions. J. Electrochem. Soc. 124,1240–1242, *DOI*: https://doi.org/10.1149/1.2133537 (1977).

19. Tachez, M., Malugani, J. P., Mercier, R., & Robert, G., Ionic conductivity of and phase transition in lithium thiophosphate Li3PS4. Solid State Ionics.14,181–185, *DOI*: https://doi.org/10.1016/0167-2738(84)90097-3 *(*1984*).*
20. Amezawa, K., Maekawa, H., Tomii, Y., & Yamamoto, K., Protonic conduction and defect structures in Sr-doped LaPO4. Solid State Ionics.145,233–240, *DOI*: https://doi.org/10.1016/S0167-2738(01)00963-8 *(*2001*).*
21. Famprikis, T., *et al.*, A New Superionic Plastic Polymorph of the Na+ Conductor Na3PS4. ACS Materials Lett. 1,641–646, *DOI*: https://doi.org/10.1021/acsmaterialslett.9b00322 *(*2019*).*
22. Sorokin, N. I., Rakov, E. G., Fedorov, P. P., & Zakalyukin, R. M., Synthesis and Electrical Properties of Ammonium Fluorostannates(II). Russ. J. Appl. Chem. 76,497–499, *DOI*: https://doi.org/10.1023/A:1025685625331 *(*2003*).*
23. Charpin, P., Roux, N., & Ehretsmann, J., Fluorures doubles de magnésium et d'ammonium. C. R. Acad. Sc. Paris. 267,484–486, *(*1968*).*
24. Kieslich, G., Sun, S., & Cheetham, A. K., Solid-state principles applied to organic-inorganic perovskites: new tricks for an old dog. Chem. Sci. 5,4712–4715, *DOI*: https://doi.org/10.1039/C4SC02211D *(* 2014*).*
25. Arachi, Y., Sakai, H., Yamamoto, O., Takeda, Y., & Imanishai, N., Electrical conductivity of the ZrO2-Ln2O3 (Ln=lanthanides) system. Solid State Ionics.121,133–139, *DOI*: https://doi.org/10.1016/S0167-2738(98)00540-2 *(*1999*).*
26. Stramare, S., Thangadurai, V., & Weppner, W., Lithium Lanthanum Titanates: A Review. Chem. Mater. 15,3974–3990, *DOI*: https://doi.org/10.1021/cm0300516 *(*2003*).*
27. Mohammad, I., Chable, J., Witter, R., Fichtner, M., & Reddy, M. A., Synthesis of Fast Fluoride-Ion-Conductive Fluorite-Type Ba1-xSbxF2+x (0.1 ≤ x ≤ 0.4): A Potential Solid Electrolyte for Fluoride-Ion Batteries. ACS Appl. Mater. Interfaces. 10,17249–17256, *DOI*: https://doi.org/10.1021/acsami.8b04108 *(*2018*).*
28. Dieudonné, B., *et al.*, The key role of the composition and structural features in fluoride ion conductivity in tysonite Ce1-xSrxF3-x solid solution.Dalton Trans.46,3761–3769, *DOI*: https://doi.org/10.1039/C6DT04714A *(*2017*).*
29. Fujisaki, F., *et al.*, Mechanical synthesis and structural properties of the fast fluoride-ion conductor PbSnF4. J. Solid State Chem. 253,287–293, *DOI*: http://doi.org/10.1016/j.jssc.2017.06.007 *(*2017*).*
30. Jorgensen, J. D., Dabrowski, B., Pei, S., Richards, D. R., & Hinks, D. G., Structure of the interstitial oxygen defect in La2NiO4+$_{\delta}$. Phys. Rev. B. 40,2187–2199, *DOI*: https://doi.org/10.1103/PhysRevB.40.2187 *(*1989*).*

Figures

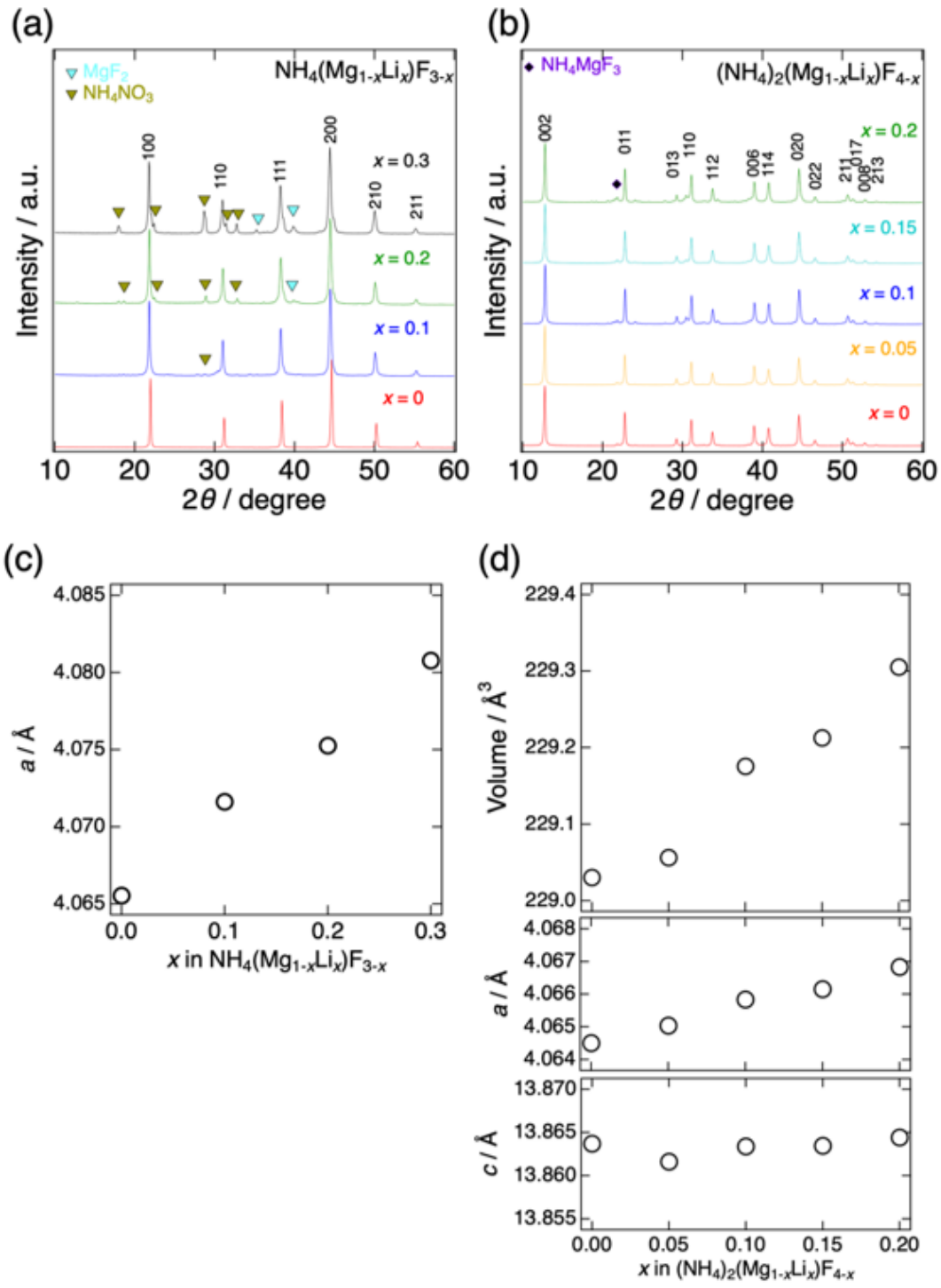

Figure 1

X-ray diffraction patterns of (a) NH4(Mg1-xLix)F3-x (x = 0, 0.1, 0.2, and 0.3) and (b) (NH4)2(Mg1-xLix)F4-x (x = 0, 0.05, 0.1, 0.15, and 0.2). Relation between the Li content and lattice parameters of (c) NH4(Mg1-xLix)F3-x and (d) (NH4)2(Mg1-xLix)F4-x. The lattice parameters were calculated assuming $Pm\bar{3}m$ structure for NH4(Mg1-xLix)F3-x and I4/mmm structure for (NH4)2(Mg1-xLix)F4-x.

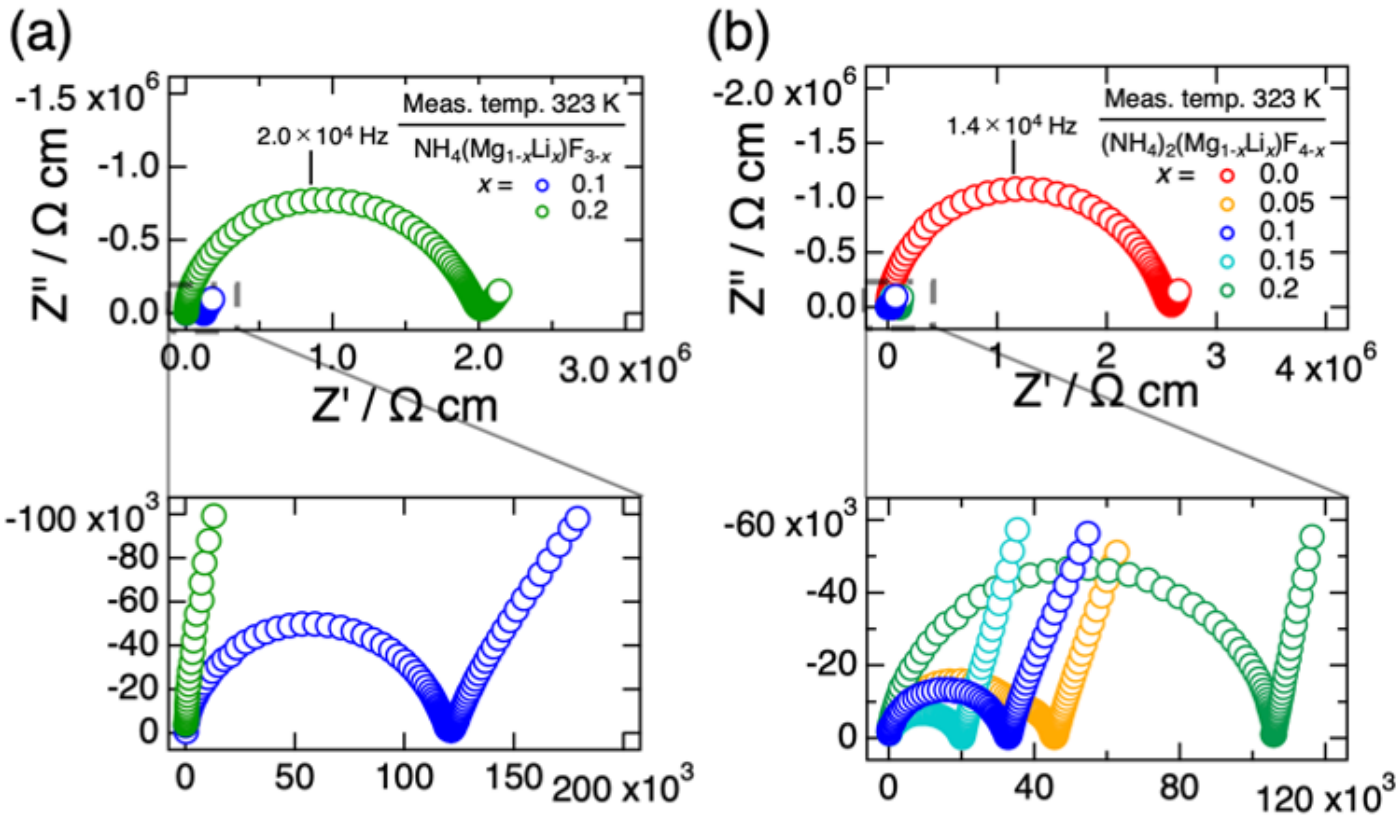

Figure 2

Nyquist plots of (a) NH4(Mg1-xLix)F3-x (x = 0.1 and 0.2) and (b) (NH4)2(Mg1-xLix)F4-x (x =0, 0.05, 0.1, 0.15, and 0.2) measured at 323 K in N2 gas.

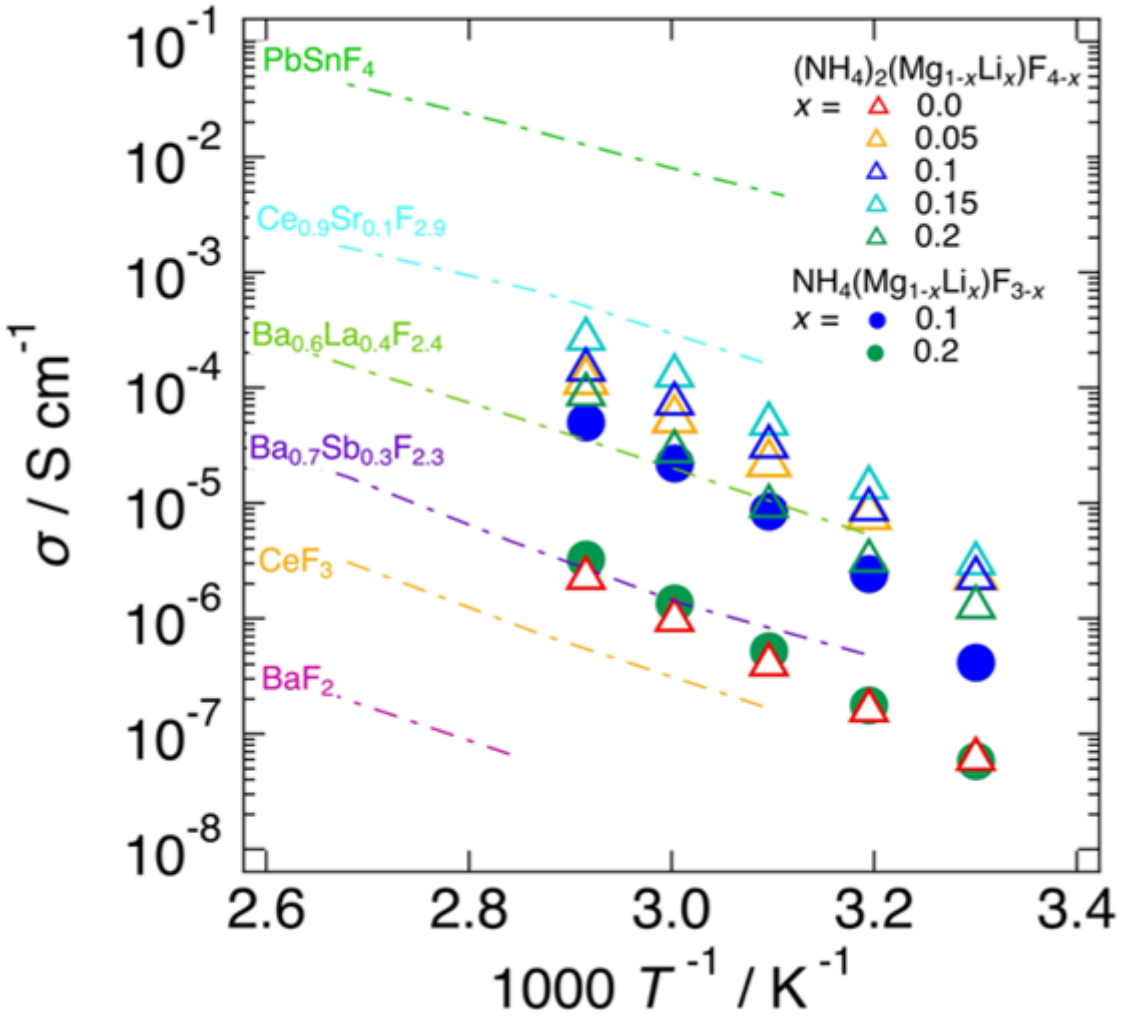

Figure 3

Temperature dependence of the electrical conductivities of NH4(Mg1-xLix)F3-x (x = 0.1 and 0.2) and (NH4)2(Mg1-xLix)F4-x (x = 0, 0.05, 0.1, 0.15, and 0.2). Reported electrical conductivities of typical fluoride ion conductors are also plotted in comparison.3, 27-29

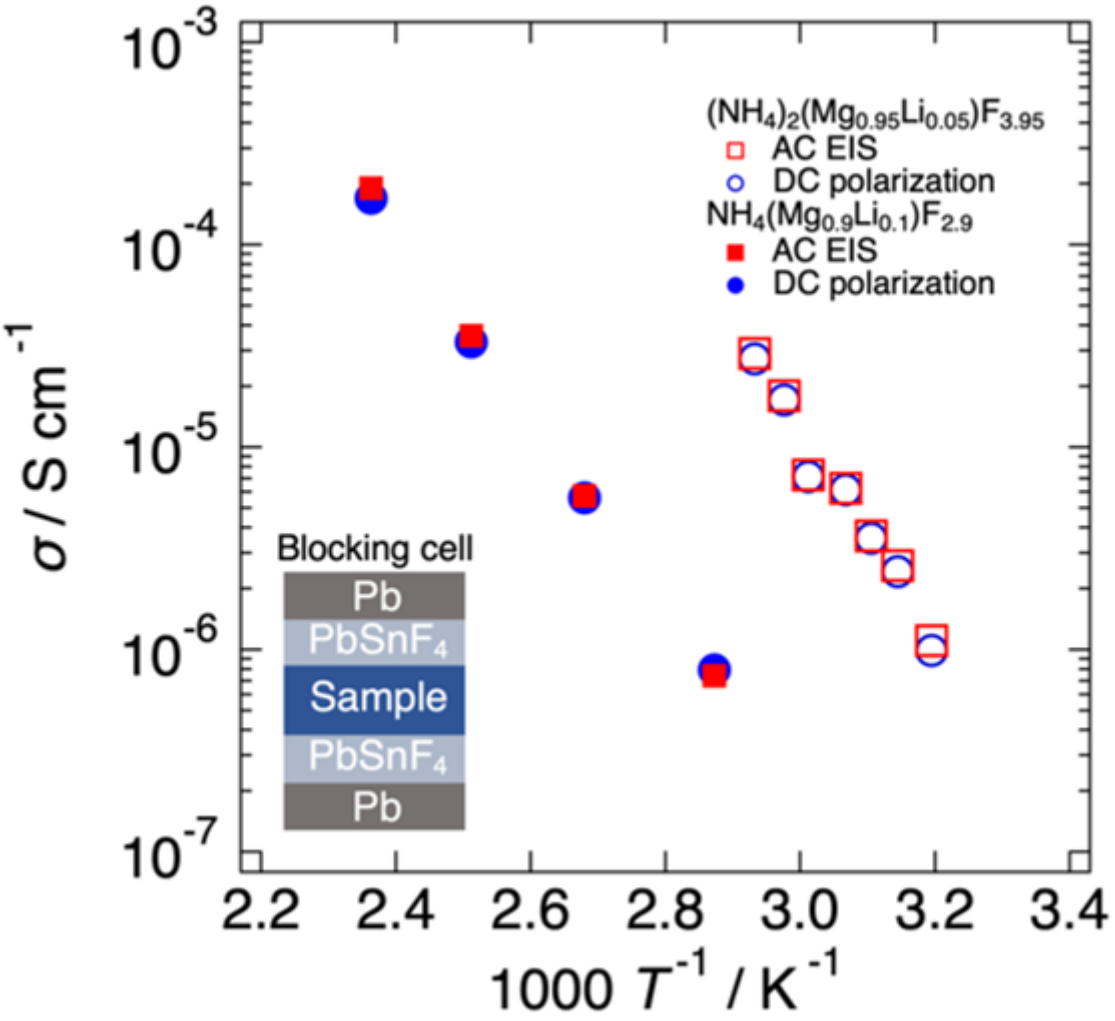

Figure 4

Temperature dependence of conductivities of NH4(Mg0.9Li0.1)F2.9 and (NH4)2(Mg0.95Li0.05)F3.95 measured by AC electrochemical impedance spectroscopy and DC polarization methods with a Pb/PbSnF4/sample/PbSnF4/Pb cell.

Supplementary Files

This is a list of supplementary files associated with this preprint. Click to download.

- SIscirepv1.docx